Cement and Concrete Research 82 (2016) 50–57

Contents lists available at ScienceDirect

Cement and Concrete Research

journal homepage: www.elsevier.com/locate/cemconres

Microstructural densification and CO_2 uptake promoted by the carbonation curing of belite-rich Portland cement

J.G. Jang, H.K. Lee *

Department of Civil and Environmental Engineering, Korea Advanced Institute of Science and Technology, 291 Daehak-ro, Yuseong-gu, Daejeon 305-701, South Korea

ARTICLE INFO

Article history:
Received 8 September 2015
Accepted 4 January 2016
Available online 17 January 2016

Keywords:
Ca_2SiO_4 (D)
Carbonation (C)
Curing (A)
Microstructure (B)
Acceleration (A)

ABSTRACT

The present study investigates the effects of the belite content and carbonation curing on the physicochemical properties of cement mortar. The results provide new insight, demonstrating that a higher belite content in cement increases CO_2 uptake during the carbonation curing process and thus promotes microstructural densification. Carbonation-cured cement with a high alite content showed increased pore connectivity, while the cement with a high belite content experienced reduced pore connectivity and more instances of pore closure, resulting in a complex microstructure. The belite phase was mostly consumed by the carbonation reaction during the curing process, resulting in the production of calcite. As a result, the mechanical strength of the carbonation-cured belite-rich Portland cement mortar was significantly improved in comparison with that after normal curing for an identical period. In particular, the reaction of the belite phase influenced by hydration/carbonation interaction at an early age is discussed along with the experimental results.

1. Introduction

Portland cement is a material consisting of the clinker minerals C_3S (referred to as alite), C_2S (mainly β-C_2S; referred to as belite), C_3A (referred to as aluminate) and C_4AF (referred to as ferrite), and a small portion of gypsum (Hereafter, the following cement chemistry nomenclature is used: C = CaO, S = SiO_2, A = Al_2O_3, F = Fe_2O_3, S= SO_3, C=CO_2 and H = H_2O). At present, C_3S in the phase composition of ordinary Portland cement accounts for 50–65% of the total proportion and critically influences the development of the concrete strength [1–3]. The hydration reaction of C_3S as expressed in Eq. (1) produces C–S–H and CH, and its rate is more rapid than that of C_2S. Significant heat generation accompanies this reaction [4].

$$C_3S + (3 + m - n)H \rightarrow C_nSH_m + (3 - n)CH. \quad (1)$$

Particular caution is warranted with regard to alite-rich cement in modern days, as it tends to increase the proportion of C_3S and is therefore associated with several issues related to the long-term durability of concrete [1,2,5–10].

On the other hand, the hydration reaction of C_2S, as expressed in Eq. (2) results in the production of CH to a lesser extent given the identical molar mass despite the reaction process being similar to that of C_3S [4].

$$C_2S + (1.5 + n)H \rightarrow C_{1.5+m}SH_{1+m+n} + (0.5 - m)CH \quad (2)$$

It is known that the hydration rate of C_2S is noticeably slower than that of C_3S owing to the different crystalline structure of these two materials [11,12]. Earlier findings regarding the hydration rate of C_2S showed slight differences depending on the study, while a quantitative X-ray powder diffraction analysis with Rietveld refinement recently conducted by Cuberos et al. showed that C_2S is not hydrated during the first three months and that the degree of the hydration reaction after one year is only 14% [13]. Nevertheless, the hydration reaction of C_2S fundamentally produces CH to a lesser extent in comparison with that of C_3S, potentially contributing to the densification and high strength development of concrete [3]. Furthermore, the optimum clinkerization temperature of belite cement is significantly lower than that of ordinary Portland cement and the amount of CO_2 generated is ~0.50 tons of CO_2 per ton of clinker, suggesting that its production demands a lower energy level and is more environmentally friendly [13–15].

Owing to these aspects, numerous studies have attempted to provide a means of overcoming the low reactivity of belite cement (c.f. [35]). These studies include an increase in the specific surface area of belite cement by means of hydrothermal technique [16]; the addition of mineral accelerators such as $CaCl_2$, $Ca(NO_3)_2$, $Ca(CH_3COO)_2$ and K_2CO_3 [12]; enhancement of the reactivity of belite by the utilization of a remelting reaction [17]; activation of the hydraulic reactivity of belite by nano-alumina [18]; the synthesis of belite cement clinkers with high hydraulic reactivity by controlling the cooling rate and with addition of mineralizers such as NaF and Fe_2O_3 [19]; and the activation of belite by doping alkaline oxides [13]. These studies commonly pay particular attention to the hydraulic reactivity of belite. Meanwhile, the carbonation reaction may provide an alternative approach by

* Corresponding author. Tel.: +82 42 350 3623; fax: +82 42 350 3610.
E-mail address: haengki@kaist.ac.kr (H.K. Lee).

http://dx.doi.org/10.1016/j.cemconres.2016.01.001
0008-8846/

which to induce a belite reaction [20,21]. Ibáñez et al. investigated the hydration and carbonation of monoclinic C_2S and C_3S by means of micro-Raman spectroscopy and found that the carbonation of hydrated C_2S is more rapid than that of hydrated C_3S exposed to an identical condition [21]. The carbonation reaction of belite present in mature cement paste has been, however, revealed to some extent thus far, while the current understanding of the reaction of the belite phase as influenced by the hydration/carbonation interaction at an early age is limited. Moreover, the effects of the carbonation of belite-rich Portland cement on physicochemical properties such as the mechanical strength, microstructure, and the degree of the reaction of hardened paste and mortar are thus far unrevealed.

Studies of CO_2 sequestration and utilization in cementitious materials are recently gaining attention (c.f. [22–25]), and carbonation curing can not only modify hardened belite-rich Portland cement but also sequestrate CO_2 into chemically stable carbonates over a long-term period. The aim of the present study is therefore to investigate the effect of the belite content and carbonation curing on the physicochemical properties of cement mortar. The mechanical strength, microstructure, reaction products and CO_2 uptake capacity are the primary topics of concern here.

2. Experimental procedure

2.1. Materials and sample preparation

Four types of Portland cement with different chemical compositions, produced from batch plants of Ssangyong Cement Industrial Co., Ltd. of South Korea, were used in this study. The chemical and physical properties of the cements are provided in Table 1. It should be noted that all cements satisfy the Portland cement specifications of Types III, I, II and IV in ASTM C150 [26]. Hence, the Blaine fineness of B16, which is classified as Type III cement with high-early strength, is different from that of the other cements. In this paper, B48 is occasionally referred to as "belite-rich Portland cement" for convenience.

Mortar specimens were fabricated with a constant mass ratio (water:cement:sand) of 1:2:3. Standard graded quartz sand was used as a fine aggregate. A cement paste specimen was fabricated with an identical w/c ratio of 0.5 to exclude the influence of the fine aggregate on the chemical analysis. Mixing was conducted for 5 min to ensure the homogeneity of the mixture. Mortar specimens were cast in a mold with dimensions of 40 × 40 × 160 mm and paste specimens were cast in a mold with dimensions of 10 × 10 × 150 mm. All specimens were sealed with plastic wrap to prevent the moisture from evaporating. They were pre-cured at 20 °C for 24 h before demolding. After demolding, the specimens were immediately placed in carbonation curing chamber.

2.2. Curing conditions and test methods

The specimen code, curing condition, and test series are summarized in Table 2. The carbonation curing was conducted in a carbonation chamber at 20 °C, RH 60% and with an atmospheric CO_2 concentration of 5%. Normally cured control specimens were provided with a condition free from carbonation in which mortar specimens for a strength test were cured at 20 °C and RH 60% and paste specimens were sealed and cured at 20 °C considering that the influence of natural carbonation on specimens of this size may be more severe.

Table 2
Summary of the test plan.

Specimen code	Curing condition	Test series[a]
B16-N	Normal curing	Series II
B23-N	(20 °C, 60 R.H.% (mortar) or sealed (paste))	Series I & II
B35-N		Series II
B48-N		Series I & II
B16-C	Carbonation curing	Series II
B23-C	(20 °C, 60 R.H.%, 5% CO_2)	Series I & II
B35-C		Series II
B48-C		Series I & II

[a] Series I involves tests of compressive strength, flexural strength and carbonation degree (using phenolphthalein indicator) using mortar specimen; and Series II involves tests of MIP, XRD and TG/DTA using paste specimen.

The experiment was systematically designed to explore the influence of carbonation curing on the carbonation degree and mechanical properties of belite-rich Portland cement mortar, along with changes in the physicochemical properties induced by carbonation curing. Series I in Table 2 is related to the former objective, and Series II is linked to the latter objective. Mortar specimens were used for Series I and paste specimens were used for Series II. The carbonation degree was measured by a phenolphthalein indicator which was sprayed onto a portion of prisms broken under a flexural strength test. Calculations were done using the ratio of the area where no color change occurred to the total cross-sectional area of the specimen. Two prism mortar specimens were tested for their flexural strength in accordance with ASTM C348. Three specimens, the portions of the prisms broken under flexure, with a cross-sectional area of 40 × 40 mm were tested for their compressive strength in accordance with ASTM C349. A universal testing machine with a loading capacity of 3000 kN was used for both tests.

Three analytical techniques were used to investigate the influence of the belite content on the changes of the physicochemical properties induced by carbonation curing. The microstructural characteristics of the normally cured and the carbonation-cured samples were evaluated by means of mercury intrusion porosimetry (MIP) on an Autopore VI 9520 machine by Micromeritics Corp. The pressure range in the MIP test was as high as 414 MPa (60,000 psi). Fractured samples at 28 days were used in the test. The hydration and carbonation products were quantified by means of thermogravimetry and differential thermal analysis (TG/DTA) using samples at 28 days. EA 1108 CHNS-O/FISONS Instruments were used; the temperature in the test was varied from 30 °C to 1000 °C with a heating rate of 30 °C/min. The clinker minerals, hydrates, and carbonation products were measured by means of X-ray diffractometry (XRD) using samples at 28 days. A SmartLab device manufactured by Rigaku was used for the XRD analysis. XRD was conducted with CuKα radiation at 40 kV and 30 mA. The scan range was 5° to 90° and the scan speed was 0.2°/min. Samples used for TG/DTA and XRD analyses were dried using desiccator and ground to pass a 100 μm sieve.

Table 1
Chemical and physical properties of the cements used in this study.

Cement	Chemical composition (wt%)						Mineral composition (wt%)[1]				Density (g/cm^3)	Blaine (cm^2/g)
	CaO	SiO_2	Al_2O_3	Fe_2O_3	SO_3	R_2O	C_3S	C_2S	C_3A	C_4AF		
B16	62.1	19.7	5.9	3.0	4.2	0.6	59	16	12	8	3.12	4400
B23	62.5	21.0	5.9	3.2	2.1	0.8	49	23	10	9	3.15	3300
B35	63.4	23.3	3.9	3.6	1.9	0.6	42	35	5	12	3.17	3350
B48	62.5	25.3	3.1	3.6	2.0	0.5	31	48	3	11	3.20	3400

[1] The mineral composition is calculated from the Bouge's equations.

3. Results and discussion

3.1. Carbonation degree and mechanical strength of belite-rich Portland cement mortar

The carbonation degree of B23-C and B48-C measured by means of a phenolphthalein indicator is shown in Fig. 1. The ratio of the carbonated area (indicated by the area where no color change occurred in Fig. 1) to the total cross-sectional area of the specimen was used to represent the carbonation degree. The carbonation degree of B23-C, made with ordinary cement, constantly increased until 14 days, while the rate decreased thereafter, resulting in 77% of the total area being carbonated at 28 days. In contrast, the carbonation degree of B48-C, made with belite-rich Portland cement, constantly increased at all ages, resulted in 92% of the total area being carbonated at 28 days.

The mechanical strengths of the normally cured or carbonation-cured B23 and B48 are shown in Fig. 2. The flexural and compressive strengths of B48-N with a high belite content were lower in comparison to those of B23-N, showing close agreement with generally known results. On the other hand, carbonation curing resulted in a remarkable increase in the flexural and compressive strengths of B23-C and B48-C. The flexural and compressive strengths of B23-C at 28 days were 11.73 MPa and 75.22 MPa, showing an increase by 165% and 124% in comparison to those of B23-N. This observation is similar to the previous works which reported the hydration reaction of ordinary Portland cement being promoted by carbonation curing [24,25]. It is, however, important to note the dramatic increase in the strength of the carbonation-cured B48; the flexural and compressive strengths of B48-C at 28 days were 14.72 MPa and 97.85 MPa, showing an increase by 197% and 172%, respectively, in comparison with those of B48-N. It is evidenced by the result obtained with the belite-rich Portland cement mortar that the degree of the reaction of belite-rich Portland cement, including hydration and carbonation, is promoted by carbonation curing.

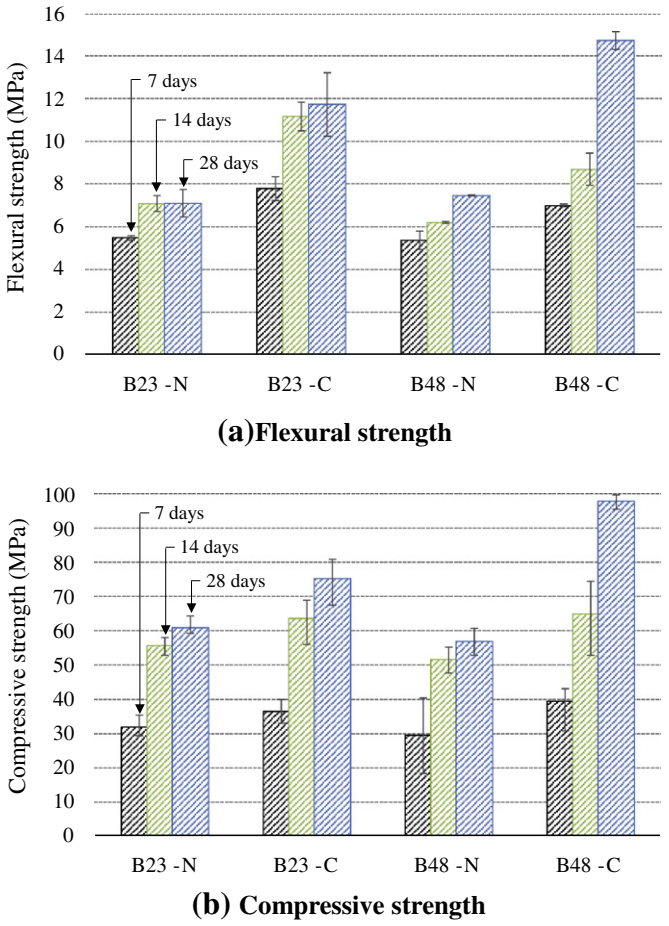

Fig. 2. Mechanical strengths of the normally cured ('N') or carbonation-cured ('C') B23 and B48: (a) flexural strength and (b) compressive strength.

3.2. Microstructure

The MIP test results of the normally cured and carbonation-cured cement paste with various belite contents are shown in Fig. 3. The

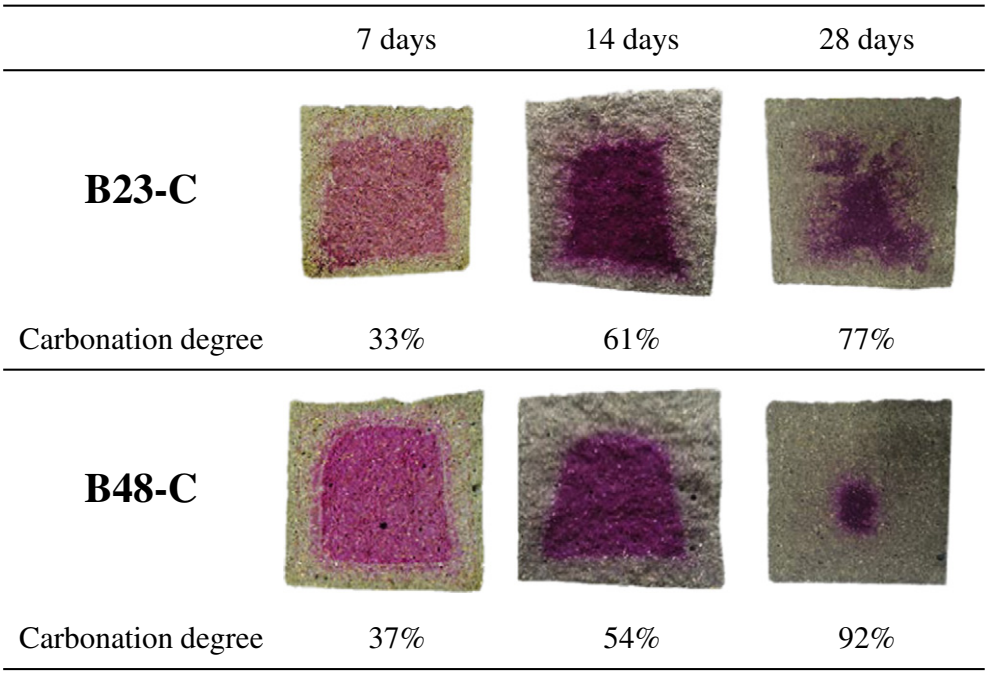

Fig. 1. Carbonation degree of B23-C and B48-C measured by means of a phenolphthalein indicator.

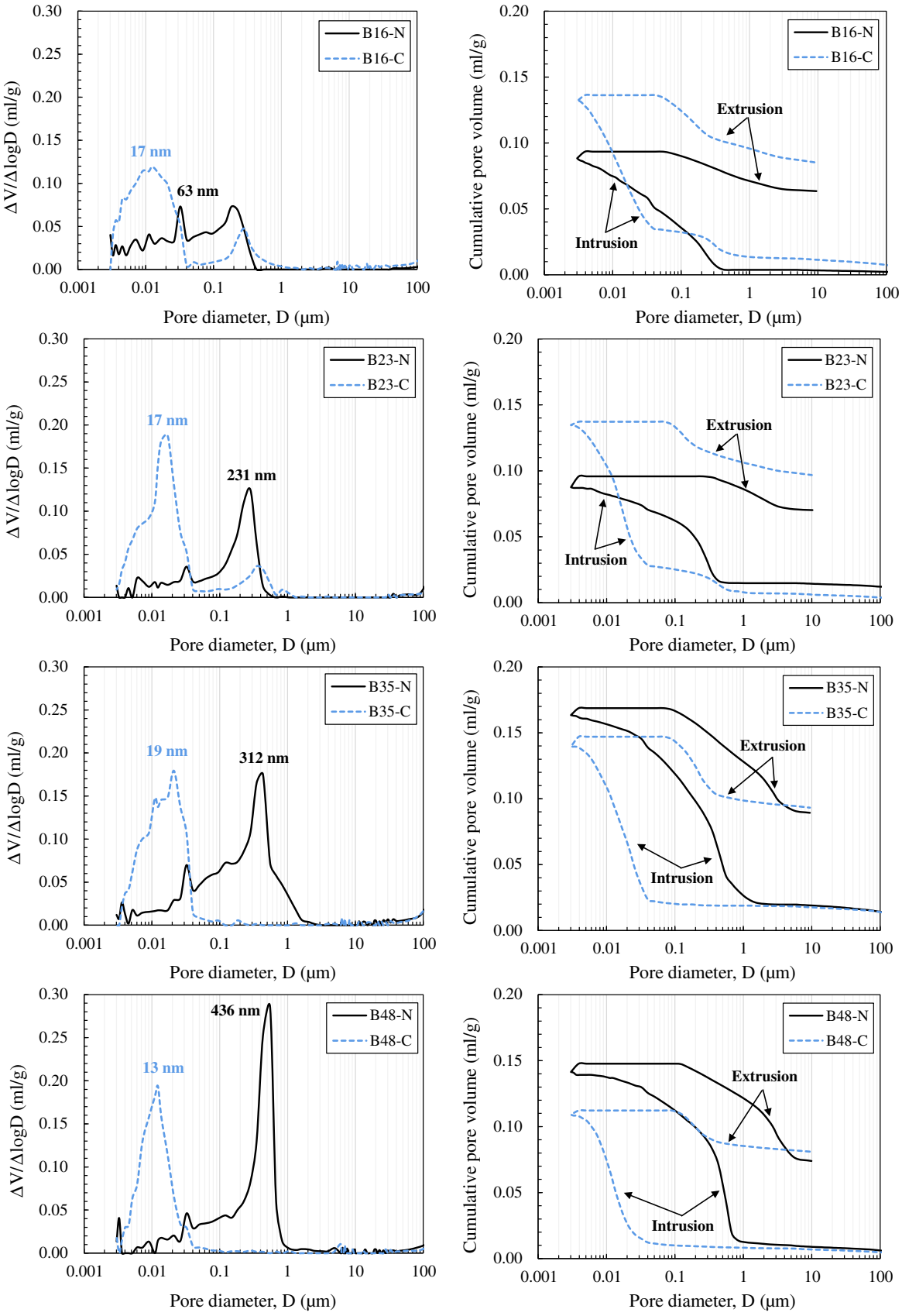

Fig. 3. MIP test results of the normally cured and carbonation-cured cement paste with various belite contents.

pore size distribution of the normally cured samples on the left in Fig. 3 indicates that the median pore diameter and pore volume at the point were proportional to the belite content. Although the strength test conducted in the present study was limited to B23 and B48, the strength result was well correlated with the pore volume when it was distributed between 50 nm and 10 μm according to the MIP results, which is known to have a critical influence on the strength and durability of a cementitious material [27,28]. The influence of carbonation as observed here was that carbonation clearly reduced the median pore diameter. For B48-C, which exhibited a remarkable increase in strength in particular, a shift of the pore size distribution to a lower diameter range was noted. Furthermore, the disappearance of median pores with diameters of 0.1 μm–1 μm in the B35-C and B48-C samples and the presence of those pores in B16-C and B23-C in contrast were noted, despite the carbonation-curing used on these samples. The cumulative pore volume was increased by carbonation curing in B16 and B23, while the opposite was true in B35 and B48, as shown on the right-hand side of Fig. 3.

The pressurization–depressurization of MIP gives the intrusion–extrusion history curve of mercury. The connectivity and structure of the pores can be evaluated by the extrusion behavior observed during the depressurization of mercury [29–31]. In general, the history curve during depressurization with a shape similar to that during pressurization indicates a low content of discontinuous ink-bottle pores and high pore connectivity of the hardened cement paste [30]. The pore diameter and amount of extruded mercury where the extrusion initiated in Fig. 3 were influenced by the belite content and by the carbonation curing process. The pore diameter range present in the specimens as revealed by mercury extrusion during the depressurization process is shown in Fig. 4 along with the general pore size distribution of the hydrated cement paste. The influence of carbonation curing on the pore diameter range where mercury extrusion occurs was prominent, while the degree of the influence varied with the belite content. The pore diameter range of B16-C and B23-C with a high alite content became broader, while the diameter and range of B35-C and B48-C with a high belite content clearly decreased. This result indicates that carbonation curing increased the pore connectivity of B16 and B23 while decreasing that of B35 and B48. Furthermore, the pore diameter as discovered by mercury extrusion plausibly elucidates the microstructures of B35-C and B48-C, which were densified and complex.

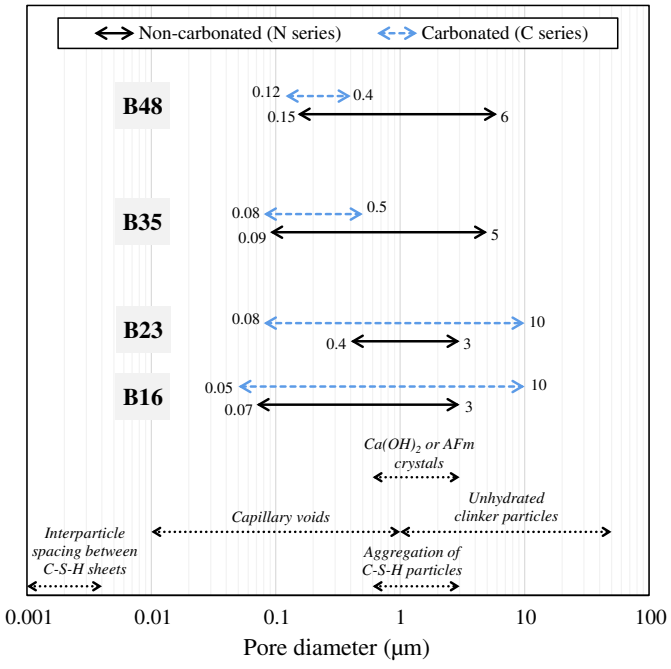

Fig. 4. Pore diameter range present in the specimens as revealed by mercury extrusion during the depressurization process: The pore size distribution of hydrated cement paste refers to that found in [3].

The amount of extruded mercury during depressurization process shown in Table 3 exhibited a trend similar to that associated with the pore diameter range as revealed by mercury extrusion in Fig. 4. The amount of extruded mercury substantially decreased in B35-C and B48-C, with a high belite content, suggesting the discontinuity of pores and a densified structure. This effect was most prominent in B48, which had the highest belite content.

3.3. XRD analysis results

XRD patterns of alite, belite, CH and calcite are shown in Fig. 5. The following 2θ values were analyzed, as the peaks at those values are essentially free from the peak overlapping: 51.7° for alite, 31.1° for belite, 34.1° for CH, and 39.4° for calcite [32]. The peak intensity of alite increased from B48 to B16 and was proportional to the alite content of each type of cement. The peak corresponding to alite was not observed in the normally cured N series or the carbonation-cured C series, indicating that alite was fully consumed. The peak intensity of belite decreased from B48 to B16 and was also proportional to the belite content of each type of cement. The peak intensity of belite in the N series was apparently reduced and was lower than that in the raw cement, though the peak still existed. The hydration reactivity of the belite phase as calculated by the Rietveld refinement method was approximately 30% regardless of the type of cement. This observation is in good agreement with the findings of previous studies, which reported relatively low hydraulic reactivity of the belite phase in comparison with that of the alite phase. Meanwhile, the peak intensity of the belite phase in the C series was lower than that in the N series and in the raw cement. The reaction degree of the belite phase as calculated by the Rietveld refinement method was approximately 90% regardless of the type of cement. The results obtained in the present study are evidences showing that the reactivity of the belite phase is promoted by carbonation curing.

The peaks corresponding to CH and calcite were only observed in the N and C series, respectively. In particular, the peak intensity of CH decreased as the belite content increased, contributing to the low hydraulic reactivity of the belite phase. On the other hand, the peak intensity of calcite increased with the belite content. A quantitative analysis of CH and calcite is discussed in the section which details the TG/DTA results.

3.4. TG/DTA results

The TG/DTA results for the normally cured and the carbonation-cured cement paste samples with various belite contents are shown in Fig. 6. An endothermic reaction peak was observed at 490 °C in the DTA curve for the N series and at 810 °C for the C series, indicating the formation of CH and CC by hydration and carbonation, respectively. The CH and CC content were quantified by the weight loss in the two regions where an endothermic reaction occurs, as presented in Fig. 6. The CH content in the non-carbonated N series decreased as the belite content was increased, showing a strong correlation. This was attributed to the hydraulic reactivity of alite phase being higher than that of the belite phase and to the fact that the hydration of the alite phase results in a higher amount of CH as compared to that of the belite phase given

Table 3
Amount of extruded mercury during the depressurization process.

(mL/kg)	Normally-cured (N series): 'A'	Carbonation-cured (C series): 'B'	'A' − 'B'
B16	30.00	51.15	−21.15
B23	25.58	40.41	−14.83
B35	79.42	53.81	25.61
B48	73.73	31.33	42.40

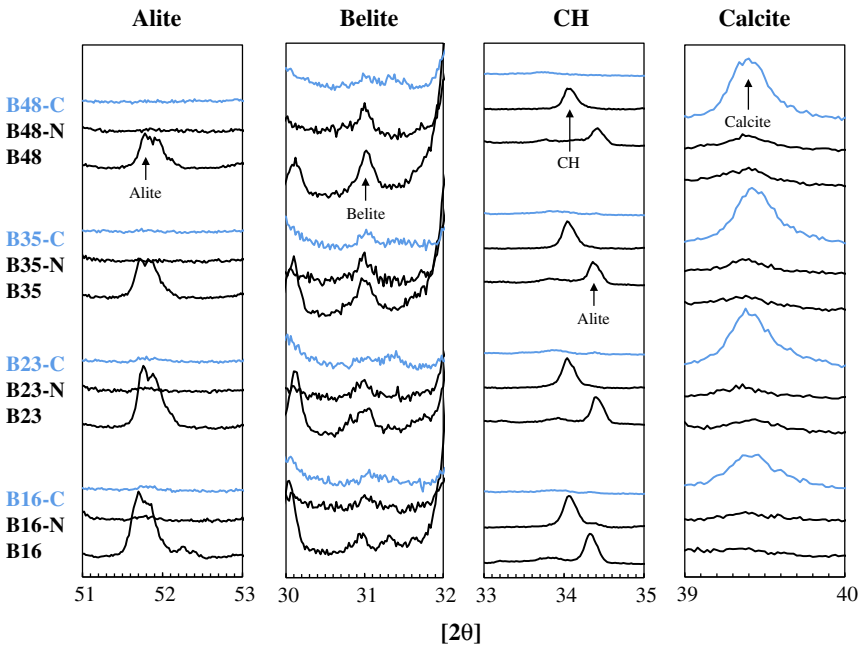

Fig. 5. XRD patterns of alite, belite, CH and calcite.

the identical molar mass, as evidenced in Eqs. (1)–(2). On the other hand, the CC content increased with the belite content.

The carbonation reaction of CH in hardened cement paste can be expressed by Eq. (3), though this may lead to the faulty conclusion that a sample with a higher CH content, B16 in this case, results in higher production of CC [33].

$$Ca(OH)_2(s\rightarrow aq) + CO_2(g\rightarrow aq)\rightarrow CaCO_3(aq\rightarrow s) + H_2O(aq) \quad (3)$$

The CC content in the carbonation-cured cement paste, however, showed an opposite result. An identical outcome was obtained according to the XRD peak patterns. The CH content in B16-N was 15.8 wt% and was the highest, while the CC content of B16-C was 18.8 wt% and was the lowest. On the other hand, B48, with the highest belite content, showed a result opposite to that observed with B16; the CH content in B48-N was 10.7 wt% and was the lowest, while the CC content in B48-C was 24.5 wt% and was the highest. This is indicative of the irrelevance of the CO_2 uptake capacity of carbonation-cured cement paste to the CH content, which is mainly determined by the alite content in a clinker. Furthermore, such phenomena were attributed to the low hydration rate of the belite phase, which reacts during the course of carbonation curing. This reaction presumably accompanies the production of CC in large amounts.

The CO_2 uptake capacity of carbonation-cured cement was calculated by Eq. (4).

$$CO_2 \text{ uptake capacity } (\%) = M_{CO_2}/M_{cement} \times 100 \quad (4)$$

Here, M_{CO_2} is the mass of CO_2 sequestrated during the course of carbonation curing, and M_{cement} is the mass of the cement used. M_{CO_2}, used to calculate the CO_2 uptake capacity, was obtained from the TG/DTA result in the present study. The calculated CO_2 uptake capacities of B16, B23, B35 and B48 were found to be 13.0%, 13.5%, 15.7% and 16.9%, respectively, showing proportionality with the belite content.

3.5. Discussion

The results obtained in the present study provide new insight, showing that a higher belite content in cement increases CO_2 uptake during carbonation curing, thus promoting microstructural densification. The belite phase, despite possessing low hydraulic reactivity, was mostly consumed by the carbonation reaction during the process, resulting in the production of calcite. In addition, the mechanical strength of belite-rich Portland cement mortar cured by carbonation for 28 days was significantly improved in comparison with that normally cured for an identical period. A schematic representation of the microstructural densification mechanism of belite-rich Portland cement by carbonation curing is shown in Fig. 7.

An interesting outcome regarding the influence of carbonation curing on the microstructure of belite-rich Portland cement was obtained in the MIP test. Carbonation-cured cement with a high alite content showed an increased amount of pore connectivity while that with a high belite content showed reduced pore connectivity and with more instances of pore closure, resulting in a complex microstructure (see Figs. 3–4 and Table 3). It is generally accepted that the hydration of cement is governed by topochemical or through-solution reaction mechanisms [4]. That is, the hydration reaction initiates at the outermost layer of a cement particle in direct contact with water, meaning that unreacted clinker minerals will most likely be located within the hydration products (mainly C–S–H) in a 3D structure [4]. Meanwhile, an interfacial transition zone exists between unreacted clinker minerals and hydration products [36]. The rate at which the hydration of the alite phase occurs is relatively rapid in comparison with that of the belite phase owing to the hydrolysis reaction of the excessively incorporated CaO in relation to SiO_2, which occurs at a rapid rate [34]. Belite, on the other hand, is relatively chemically stable and its lower hydraulic reactivity therefore can be assumed to result in the large interfacial transition zone with a large specific surface area between unreacted clinker minerals and hydration products during the course of the hydration reaction [37]. The diffusivity of CO_2 in a porous medium is higher than that of H_2O due to the diffusivity in a gaseous state being higher than that in an aqueous state. Accordingly, the rate of the carbonation reaction occurring at the inner layer of the hydrated C–S–H and the outer layer of an unreacted belite particle is likely to be more rapid than that of the hydration reaction. The consequence of this interaction results in the densification of the microstructure, consisting of aggregated C–S–H particles – capillary voids – interparticle spacing between C–S–H sheets, as well as reductions of the pore volume and connectivity.

On the other hand, the XRD and TG/DTA results indicate that the carbonation reaction can be promoted by increasing the belite content.

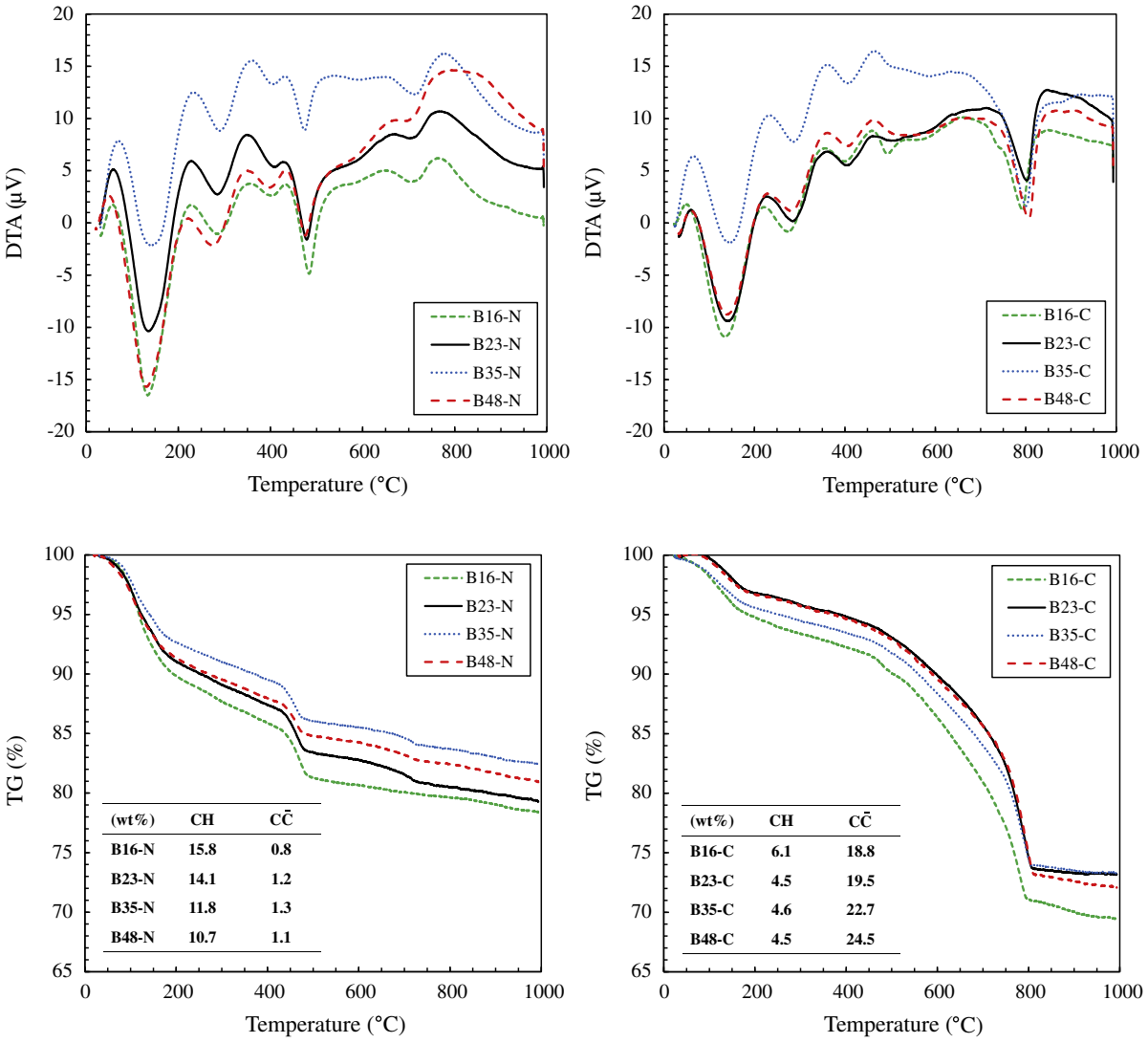

Fig. 6. TG/DTA results for the normally cured and the carbonation-cured cement paste samples with various belite contents.

The changes in the hydrates and the microstructure induced by carbonation curing stand in contrast to the carbonation behavior of mature cement paste (i.e., consumption of CH and partially C–S–H, resulting in production of CC), due most likely to the initiation of carbonation at a significantly early age and because the pore solution is saturated by CO_3^{2-} at a high concentration. Carbonation curing in the present study started 24 h after placement, as a large number of ions released from the cement were dissolved in the pore solution at this point [4]. In this context, carbonation curing results in the pore solution of cement paste at an early age being saturated with CO_3^{2-}. Ca^{2+} ions dissociated from the cement participate in the production of C–S–H and simultaneously react with either OH^- or CO_3^{2-}. Meanwhile, the amount of

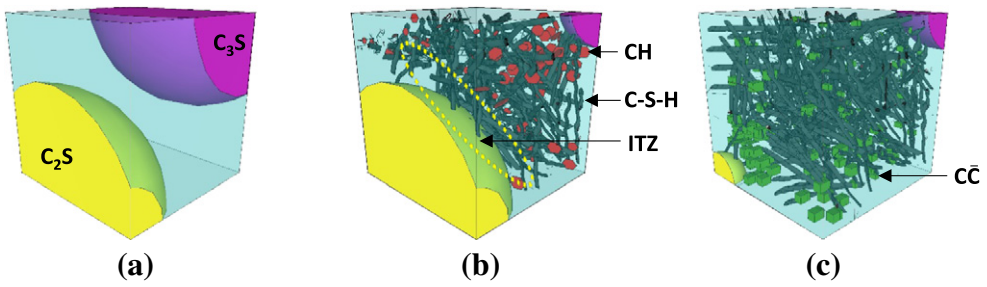

Fig. 7. Schematic representation of the microstructural densification mechanism of belite-rich Portland cement by carbonation curing. (a): Unhydrated alite and belite particle are schematically drawn. (b): The formation of C–S–H and CH by hydration is presented. Alite with a high hydraulic reactivity, is mostly consumed in the hydration while belite with a low hydraulic reactivity is only slightly consumed, majority remaining unhydrated. Furthermore, an interfacial transition zone (ITZ) with a low density of hydrates resides between unhydrated belite particle and C–S–H produced by hydration of the alite. (c): Change in the hydrates induced by carbonation curing is schematically presented. Carbonation curing induces the dissolution of the belite phase into the pore solution and the production of CC in the pore solution saturated with CO_3^{2-}. This reaction is effective to reduce the amount of ITZ between the inner layer of hydrated C–S–H and the outer layer of unreacted belite particle, which in turn densifies the microstructure.

Ca^{2+} which can react with those two anions is low in belite-rich Portland cement with a low alite content, leading to the dissolution of the belite phase into the pore solution. The location of such a reaction is not only limited to the capillary pores where carbonation occurs in mature cement paste but also transpires at the interfacial transition zone between the inner layer of the hydrated C–S–H and the outer layer of the unreacted belite particle, ultimately resulting in the microstructural densification of pores in a range of 50 nm to 10 μm, thus having a significant influence on the strength.

4. Conclusions

The present study investigates the effects of belite content and carbonation curing on the physicochemical properties of cement mortar. The results obtained in this study provide a new insight showing that a higher belite content in cement increases CO_2 uptake during the carbonation curing process, thus promoting microstructural densification. The main conclusions extracted from this work are as follows.

(1) The MIP results showed that carbonation-cured cement with a high alite content demonstrated increased pore connectivity, while that with a high belite content showed reduced pore connectivity and more instances of pore closure, resulting in a complex microstructure.
(2) XRD and TG/DTA results showed that the belite phase was mostly consumed by the carbonation reaction during the curing process, resulting in the production of calcite. The CO_2 uptake capacities of B16, B23, B35 and B48 were 13.0%, 13.5%, 15.7% and 16.9%, respectively, showing proportionality with the belite content.
(3) The mechanical strength of the carbonation-cured belite-rich Portland cement mortar was significantly improved in comparison with that normally cured for an identical period.
(4) The location of such a reaction is not only limited to the capillary pores where carbonation occurs in matured cement paste but also arises at the interfacial transition zone between the inner layer of the hydrated C–S–H and the outer layer of unreacted belite particles, ultimately resulting in the microstructural densification of pores in the range of 50 nm to 10 μm, which significantly influences the strength.

Acknowledgments

This study was supported by the Saudi Aramco—KAIST CO_2 Management Center to whom the authors are grateful. The authors would like to thank Mr. Sol-Moi Park, Mr. Geun-U Ryu and Ms. Hee-Jeong Kim at KAIST for their cooperation in this study.

References

[1] A. Neville, Maintenance and durability of structures, Concr. Int. 19 (1997) 52–56.
[2] P.K. Mehta, R.W. Burrows, Building durable structures in the 21st century, Concr. Int. 23 (2001) 57–63.
[3] P.K. Mehta, P.J.M. Monteiro, Concrete: Microstructure, Properties, and Materials, third ed. McGraw-Hill, 2006.
[4] P.C. Hewlett, Lea's Chemistry of Cement and Concrete, Butterworth-Heinemann, Oxford, U.K., 1998
[5] Rasheeduzzafar, Influence of cement composition on concrete durability, ACI Mater. J. 89 (1992) 574–586.
[6] S.A. Altoubat, D.A. Lange, Creep, shrinkage, and cracking of restrained concrete at early age, ACI Mater. J. 98 (2001) 323–331.
[7] G.D. Schutter, Finite element simulation of thermal cracking in massive hardening concrete elements using degree of hydration based material laws, Comput. Struct. 80 (2002) 2035–2042.
[8] J. Marchand, D.P. Bentz, E. Samson, Y. Maltais, Influence of calcium hydroxide dissolution on the transport properties of hydrated cement systems, in: J. Skalny, J. Gebauer, I. Odler (Eds.),Materials Science of Concrete: Calcium Hydroxide in Concrete, Special Volume 2001, pp. 113–129.
[9] F.P. Glasser, J. Marchand, E. Samson, Durability of concrete—degradation phenomena involving detrimental chemical reactions, Cem. Concr. Res. 38 (2008) 226–246.
[10] M. O'Connell, C. McNally, M.G. Richardson, Biochemical attack on concrete in wastewater applications: a state of the art review, Cem. Concr. Compos. 32 (2010) 479–485.
[11] S.M. Ghosh, P.B. Rao, A.K. Paul, K. Raina, The chemistry of dicalcium silicate mineral, J. Mater. Sci. 14 (1979) 1554–1566.
[12] H. El-Didamony, A.M. Sharara, I.M. Helmy, S. Abd El-Aleem, Hydration characteristics of β-C_2S in the presence of some accelerators, Cem. Concr. Res. 26 (1996) 1179–1187.
[13] A.J.M. Cuberos, Á.G. De la Torre, M.C. Martín-Sedeño, L. Moreno-Real, M. Merlini, L.M. Ordónez, M.A.G. Aranda, Phase development in conventional and active belite cement pastes by Rietveld analysis and chemical constraints, Cem. Concr. Res. 39 (2009) 833–842.
[14] C.D. Popescu, M. Muntean, J.H. Sharp, Industrial trial production of low energy belite cement, Cem. Concr. Compos. 25 (2003) 689–693.
[15] T. Staněk, P. Sulovský, Active low-energy belite cement, Cem. Concr. Res. 68 (2015) 203–210.
[16] H. Ishida, K. Mabuchi, K. Sasaki, T. Mitsuda, Low-temperature synthesis of β-Ca_2SiO_4 from hillebrandite, J. Am. Ceram. Soc. 75 (1992) 2427–2432.
[17] K. Fukuda, N. Wakamatsu, S. Ito, H. Yoshida, Acceleration of early hydration in belite-rich cement by remelting reaction, J. Ceram. Soc. Jpn. 107 (1999) 901–906.
[18] I. Campillo, A. Guerrero, J.S. Dolado, A. Porro, J.A. Ibáñez, S. Goñi, Improvement of initial mechanical strength by nanoalumina in belite cements, Mater. Lett. 61 (2007) 1889–1892.
[19] L. Kacimi, A. Simon-Masseron, S. Salem, A. Ghomari, Z. Derriche, Synthesis of belite cement clinker of high hydraulic reactivity, Cem. Concr. Res. 39 (2009) 559–565.
[20] C.J. Goodbrake, J.F. Young, R.L. Berger, Reaction of beta-dicalcium silicate and tricalcium silicate with carbon dioxide and water vapor, J. Am. Ceram. Soc. 62 (1979) 168–171.
[21] J. Ibáñez, L. Artús, R. Cuscó, Á. López, E. Menéndez, M.C. Andrade, Hydration and carbonation of monoclinic C_2S and C_3S studied by Raman spectroscopy, J. Raman Spectrosc. 38 (2007) 61–67.
[22] I. Galan, C. Andrade, P. Mora, M.A. Sanjuan, Sequestration of CO_2 by concrete carbonation, Environ. Sci. Technol. 44 (2010) 3181–3186.
[23] S. Monkman, Y. Shao, Integration of carbon sequestration into curing process of precast concrete, Can. J. Civil Eng. 37 (2010) 302–310.
[24] V. Rostami, Y. Shao, A.J. Boyd, Z. He, Microstructure of cement paste subject to early carbonation curing, Cem. Concr. Res. 42 (2012) 186–193.
[25] V. Rostami, Y. Shao, A.J. Boyd, Carbonation curing versus steam curing for precast concrete production, J. Mater. Civil Eng. 24 (2012) 1221–1229.
[26] American Society for Testing and Materials, ASTM C150/C150M—12: Standard specification for Portland cement, ASTM international, 2012.
[27] V.T. Ngala, C.L. Page, Effect of carbonation on pore structure and diffusional properties of hydrated cement pastes, Cem. Concr. Res. 27 (1997) 995–1007.
[28] D.A. Silva, V.M. John, J.L.D. Ribeiro, H.R. Roman, Pore size distribution of hydrated cement pastes modified with polymers, Cem. Concr. Res. 31 (2001) 1177–1184.
[29] S. Diamond, Mercury porosimetry: an inappropriate method for the measurement of pore size distributions in cement-based materials, Cem. Concr. Res. 30 (2000) 1517–1525.
[30] F. Moro, H. Böhni, Ink-bottle effect in mercury intrusion porosimetry of cement-based materials, J. Colloid Interf. Sci. 246 (2002) 135–149.
[31] J. Zhou, G. Ye, K. van Breugel, Characterization of pore structure in cement-based materials using pressurization–depressurization cycling mercury intrusion porosimetry (PDC-MIP), Cem. Concr. Res. 40 (2010) 1120–1128.
[32] P.E. Stutzman, Guide for X-ray powder diffraction analysis of Portland cement and clinker, National Institute of Standards and Technology, NISTIR, 5755 1996, pp. 1–38.
[33] M.A. Peter, A. Muntean, S.A. Meier, M. Böhm, Competition of several carbonation reactions in concrete: a parametric study, Cem. Concr. Res. 38 (2008) 1385–1393.
[34] M.E. Tadros, J. Skalny, R.S. Kalyoncu, Early hydration of tricalcium silicate, J. Am. Ceram. Soc. 59 (1976) 344–347.
[35] H.-M. Ludwig, W. Zhang, Research review of cement clinker chemistry, Cem. Concr. Res. 78 (2015) 24–37.
[36] K.L. Scrivener, Backscattered electron imaging of cementitious microstructures: understanding and quantification, Cem. Concr. Compos. 26 (2004) 935–945.
[37] I.G. Richardson, The nature of C–S–H in hardened cements, Cem. Concr. Res. 29 (1999) 1131–1147.